bioRxiv preprint doi: https://doi.org/10.1101/2022.12.12.520161; this version posted December 13, 2022. The copyright holder for this preprint (which was not certified by peer review) is the author/funder, who has granted bioRxiv a license to display the preprint in perpetuity. It is made available under aCC-BY-NC-ND 4.0 International license.

Regulation of neuroinflammation by astrocyte-derived cholesterol.

Hao Wang[1,2,3,^], Joshua A. Kulas[4,5,^], Holden Higginbotham[6], Michael A. Kovacs[5], Heather A. Ferris[4,5*], Scott B. Hansen[1,2*]

[1]Department of Molecular Medicine, [2]Department of Neuroscience, [3]Skaggs Graduate School of Chemical and Biological Sciences, The Scripps Research Institute, Jupiter, FL 33458, USA
[4]Division of Endocrinology and Metabolism, [5]Center for Brain Immunology and Glia, Department of Neuroscience, University of Virginia, Charlottesville, VA 22908, USA
[6]Department of Biology, Brigham Young University-Idaho, Rexburg, ID 83460, USA.
^HW and JAK contributed equally to this work.
*Correspondence: shansen@scripps.edu or hf4f@virginia.edu

Abstract

Neurodegeneration and its concomitant loss of cognitive function is associated with inflammation and an accumulation of lipids, in particular cholesterol. In the brain, cholesterol is made in astrocytes and transported to surrounding cells by apolipoprotein E (apoE). Elevated cholesterol promotes inflammation in peripheral tissues, but whether astrocyte cholesterol can drive inflammation in the brain is unclear. Here we show that pro-inflammatory cytokines induce cholesterol synthesis in astrocytes. The astrocytes release the cholesterol and immune cells take it up, which causes clustering of proinflammatory receptors in lipid rafts, perpetuating the inflammatory signal. Knockout of cholesterol synthesis in astrocytes blocks the production of inflammatory cytokines in an AD mouse brain and reduces neuroinflammation induced by peripheral injection of lipopolysaccharide (LPS) into the mouse. We conclude that astrocyte cholesterol is a paracrine signal to microglia and tissue-resident macrophages, resulting in increased neuroinflammation.

Introduction

Neurodegeneration is a debilitating condition characterized by loss of memory and cognitive function–it is frequently associated with increased age and neuroinflammation [1]. The neuroinflammation is caused by activation of innate immunity. In healthy individuals, inflammation is acute and resolves itself, but with age, disease, or repeated injury the inflammation can become chronic [2]. Many prominent neurodegenerative diseases, including Alzheimer's disease (AD) and Parkinson's, exhibit significant features of chronic neuroinflammation [3–5]. There is also evidence that neurological complications following the resolution of COVID-19 and other infections are a result of sustained neuroinflammation[6]. The cellular and molecular mechanisms responsible for the escalation and resolution of chronic neuroinflammation are still being worked out.

At a cellular level, an interplay between astrocytes and microglia is associated with neuroinflammation [7 8 9] (see Supplemental Figure S1A-B). Microglia are the primary immune cell of the brain and they release cytokines and factors which activate astrocytes [7]. Astrocytes are the primary support cells for neurons. Astrocytes release extracellular factors which are both pro- and anti-inflammatory on microglia [7,10]. Among their many functions, astrocytes produce the majority of cholesterol in the brain, which is separate from peripheral cholesterol obtained from the liver and diet [11].

At the molecular level, clustering of inflammatory proteins drives the release of inflammatory factors [12,13] (see Supplementary Figure S1C). Cholesterol mediates this clustering. For example, cholesterol clusters toll-like receptor (TLR), triggering receptor expressed on myeloid cells 2 (TREM2), and interferon-gamma receptor (IFNγR). Clustering activates TLR4 by dimerization, while clustering activates TNFα by exposing it to its hydrolytic enzyme in a process called substrate presentation [12,14] (Supplemental Figure S1D). Their activation are major contributors to neuroinflammation [12]. A number of findings suggest a link between abnormal cholesterol metabolism and AD pathogenesis. Aged, or pro-inflammatory microglia accumulate cholesterol and other neutral lipids [15]. Despite these observations, cholesterol as a component of microglia/astrocyte communication is not well understood.

Astrocytes are known to produce and release cholesterol to nearby neurons [11,16]. We recently showed that cholesterol is an extracellular signal that when transported to neurons via apolipoprotein E (apoE) activates amyloid production and tau phosphorylation in an AD mouse model. Selectively knocking out a key cholesterol synthesis protein sterol regulatory element-binding protein 2 (SREBP2) from

bioRxiv preprint doi: https://doi.org/10.1101/2022.12.12.520161; this version posted December 13, 2022. The copyright holder for this preprint (which was not certified by peer review) is the author/funder, who has granted bioRxiv a license to display the preprint in perpetuity. It is made available under aCC-BY-NC-ND 4.0 International license.

astrocytes (SB2-/-) abolished the amyloid production and tau phosphorylation [17].

We hypothesized that astrocytes could also deliver cholesterol to nearby microglia as a signal to cluster inflammatory proteins. If so, this would establish astrocyte-derived cholesterol as a potential driver of microglial activation in neuroinflammation. Here we show that astrocyte cholesterol regulates neuro-inflammatory factors in cultured immune cells and in mouse models of inflammation and AD.

Results

Regulation of cholesterol production in astrocytes by pro-inflammatory cytokines.

Interleukin 6 (IL6) and tumor necrosis factor (TNF) alpha (TNFα) are potent cytokines that activate astrocytes [7,8]. In the periphery, cytokines promote cholesterol synthesis in hepatocytes (the primary cholesterol producing cells of the periphery) (Supplemental Figure S1B) [18]. If cytokines work in the same way in the brain, we hypothesized they would activate cholesterol synthesis in astrocytes.

To test this hypothesis, we incubated primary astrocytes with pro-inflammatory cytokines IL1β, IL6, and TNFα and measured free cholesterol (non-esterified) available in live cells (cellular and extracellular) using a fluorescent cholesterol assay. We found that inflammatory cytokines acutely (within 2 hours (h)) and dose-dependently increase the amount of free cholesterol (Figure S2A-C). IL6 had the greatest effect, increasing cholesterol by >200%, followed by TNFα (~180%), and IL1β (~20%).

To distinguish an increase in cholesterol release vs. accumulation in the membrane, we treated astrocytes with cytokines for 24hrs, removed the cytokines, and then assayed the accumulation of cholesterol in the media, separate from the cells. We refer to the media taken from astrocytes as astrocyte conditioned media (ACM). Together, extracellular cholesterol and cellular cholesterol (cell lysates) indicate the relative increase in astrocyte cholesterol production.

We found IL6 and TNFα increased both total and free cholesterol levels in ACM (Figure 1A-B). The cholesterol in the total lysate of the cells remained essentially the same (Figure 1C-D), suggesting the cells maintain a constant intracellular concentration of cholesterol while increasing the release of cholesterol into the medium (Figure 1D). Lipopolysaccharide (LPS), a positive control for inflammation, stimulated the release of similar amounts of cholesterol into the ACM.

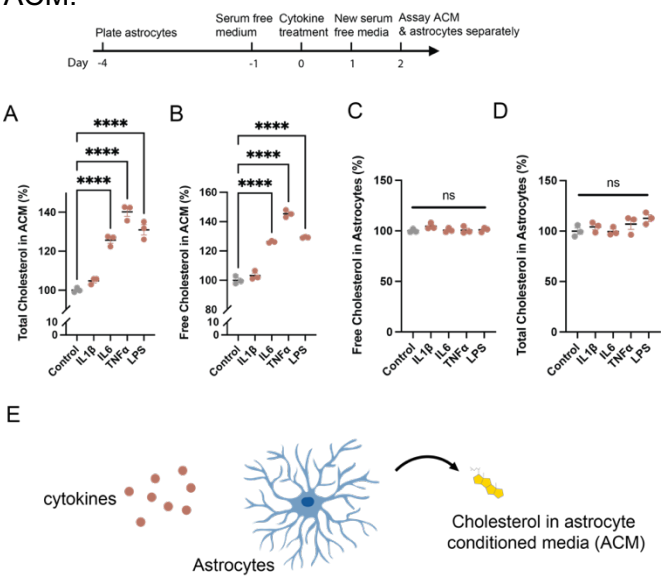

Figure 1. Inflammatory cytokines induce cholesterol release from astrocytes. Free cholesterol released into the media was measured by a fluorescent cholesterol oxidase assay. (A-B) Cholesterol released into the astrocyte conditioned media (ACM) was increased with by cytokines and lipopolysacharaide (LPS). Total cholesterol is both free cholesterol and cholesterol esters. (C-D) Cholesterol in the astrocytes was measured separate from the media. Values are expressed as mean (n= 3 wells of cells from 2 animals) done at least in duplicate (>4 animals). Comparison made with a Student's T test; *p≤0.05, ** p≤0.01, **** p≤0.0001 (E) Cartoon showing experimental setup. Cytokines (brown dots) are added to cultured astrocytes (blue shaded cell) causing release of cholesterol into the media.

Uptake of astrocyte cholesterol into immune cells.

Next we asked if the cholesterol released from the activated astrocytes is taken up into the microglia. To test our hypothesis, we activated astrocytes with a cytokine cocktail (IL1β, TNFα, and IL6), conditioned fresh media with the activated astrocytes, and then applied the ACM to a human microglia-like cell line (HCM3) and measured cholesterol uptake into the microglia. In microglia, the cytokines applied to astrocytes induced a modest and statistically significant increase in plasma membrane cholesterol levels (Figure 2A).

Macrophages are another type of immune cell in the central nervous system. Recently, macrophages have been recognized as prominent contributors to neuroinflammation [19]. Furthermore, in multiple scleroses (MS), macrophages can become trapped behind the BBB and escalate neurodegeneration [20].

bioRxiv preprint doi: https://doi.org/10.1101/2022.12.12.520161; this version posted December 13, 2022. The copyright holder for this preprint (which was not certified by peer review) is the author/funder, who has granted bioRxiv a license to display the preprint in perpetuity. It is made available under aCC-BY-NC-ND 4.0 International license.

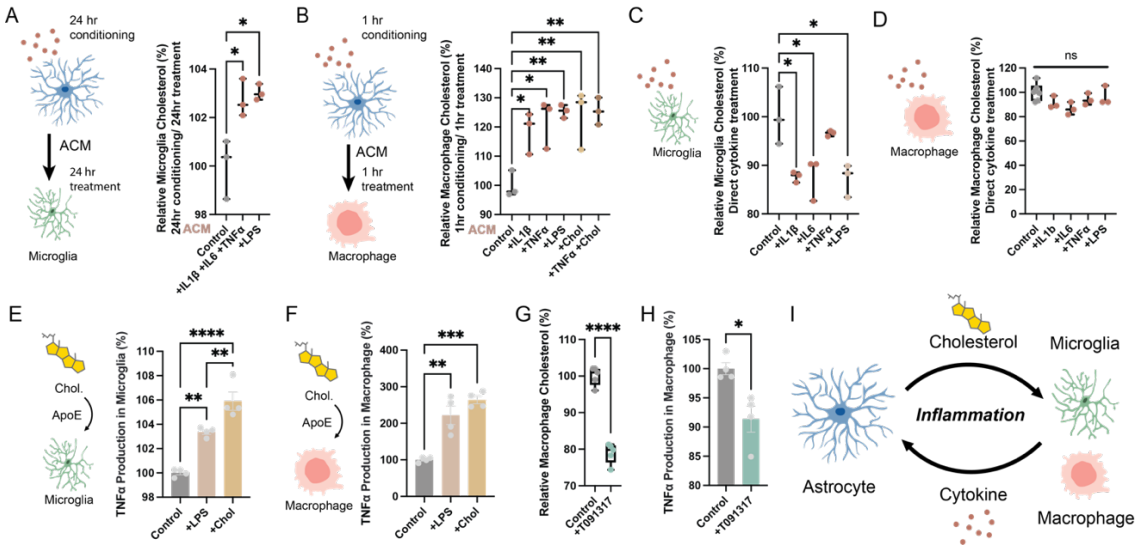

Figure 2. Cytokines signal to immune cells through astrocyte derived cholesterol. (A) A cartoon of the experimental setup is shown with cytokines (brown dots) (100 ng/mL) activating astrocytes (blue shaded cell). The cytokines were applied to astrocytes 24hr washed off and fresh media was conditioned for 24hr. The astrocyte conditioned media (ACM), without cytokines, was then transferred to microglia-like HMC3 cells (green shaded cell) and the cholesterol levels in the microglia measured. Free cholesterol was measured by a fluorescent cholesterol oxidase assay after treatment with ACM. (B) Macrophage-like RAW 264.7 cells (pink shaded cell) were treated for 1hr with ACM. (C-D) Free cholesterol levels in HMC3 microglia (C) and RAW 264.7 macrophages (D) after direct application of 100 ng/mL cytokines. (E-F) Measurement of TNF-α protein release after direct treatment of microglia (E) and macrophages (F) with cholesterol (4 ng/ml apolipoprotein E + 10% serum). Cholesterol behaved similar to 10 ng/mL LPS (positive control) in both cell types. (G-H) T091317, a Liver X receptor agonist, decreased cholesterol in macrophages, which correlated with a decreased TNF-α production in macrophage. (I) Proposed model for astrocyte cholesterol in neuroinflammation. Astrocyte-derived cholesterol induces activation of microglia and macrophages and triggers cytokine release. Cytokines and other pro-inflammatory molecules released by microglia and macrophages in turn stimulate cholesterol release from astrocytes, triggering neuroinflammation. Values are expressed as mean. In A-B, each point is a well of cells from 2 animals done at least in duplicate (>4 animals). Comparison made with a Student's T test; *p≤0.05, **p≤0.01, ***p≤0.001, ****p≤0.0001.

To test the macrophage response to astrocyte cholesterol, we treated RAW264.7 cells with ACM for 1hr. Figure 2C shows uptake of cholesterol in macrophages was extremely robust. Cellular cholesterol levels increased almost 30% (Figure 2B). This suggests that the smaller percentage of cholesterol uptake into microglia was not due to a lack of available cholesterol in the ACM (Figure 2A), rather the levels of cholesterol in macrophages appear to be more responsive or dynamic compared to microglia (Supplemental Figure S2D).

In theory, the cytokines used to activate astrocytes could contaminate the ACM and directly activate cholesterol synthesis in microglia. To confirm that our observed increase in immune cell cholesterol is from astrocytes and not from cytokine activation of microglia, we directly applied cytokines to microglia and macrophages and measured the change in cholesterol levels with our fluorescent assay. As expected, and in contrast to astrocytes, pro-inflammatory cytokines alone did not increase cholesterol in microglia or macrophages (Figure 2C-D). In fact, in microglia, IL1β and IL6 caused a small, but statistically significant decrease in cholesterol. This result suggests that the increased cholesterol in microglia in Figure 2A-B is likely exogenous cholesterol release from the astrocyte cholesterol and not denovo synthesis of cholesterol in microglia or macrophages.

Cholesterol activation of microglia and macrophages.

We previously showed the cholesterol released from astrocytes requires apoE [17]. We have also showed that purified apoE3 and 10% fetal bovine serum (FBS, an external source of cholesterol) can recapitulate the effects of high extracellular cholesterol [17,21,22]. To confirm microglia activation by apoE-mediated cholesterol uptake, we cultured HMC3 cells with apoE3 with/without FBS and measured TNFα production using an enzyme-linked immunosorbent assay (ELISA) for TNFα.

bioRxiv preprint doi: https://doi.org/10.1101/2022.12.12.520161; this version posted December 13, 2022. The copyright holder for this preprint (which was not certified by peer review) is the author/funder, who has granted bioRxiv a license to display the preprint in perpetuity. It is made available under aCC-BY-NC-ND 4.0 International license.

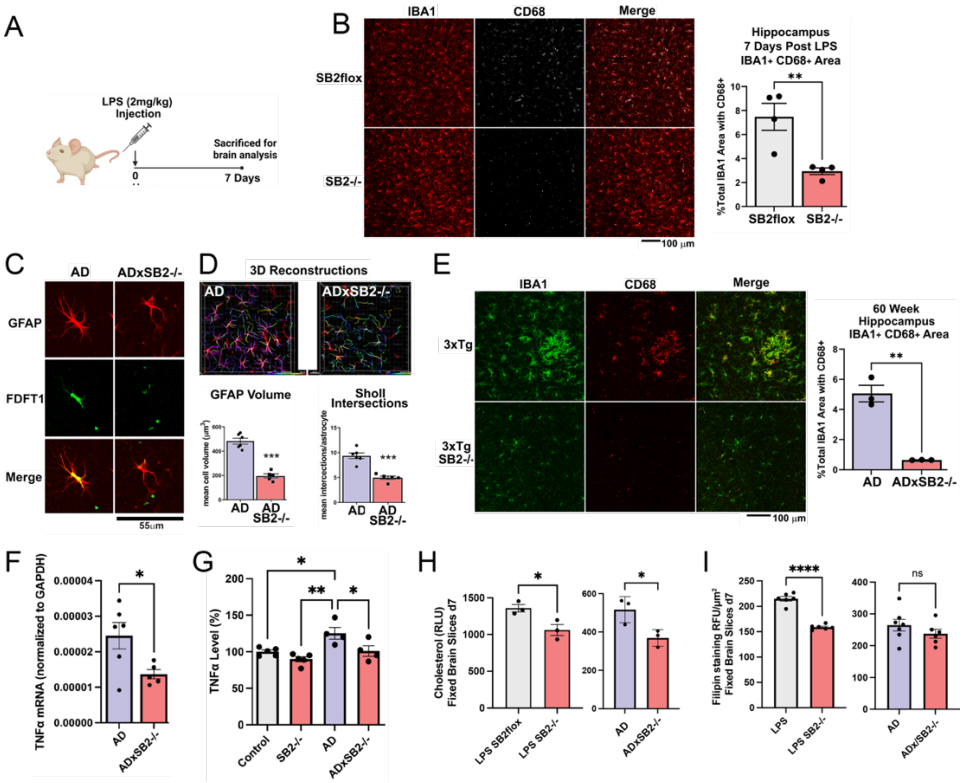

Figure 3. Decreased astrocyte cholesterol resolves neuroinflammation after peripheral LPS injection. (A, B) SREBP2 floxed mice (SB2flox) were crossed to GFAP-Cre$^{+/-}$ mice (SB2$^{-/-}$) to generate mice that do not produce cholesterol specifically in astrocytes. SB2flox (control) and SREBP2-/- mice were given 2mg/kg LPS by I.P. injection. Hippocampal microglia were assessed for CD68 content after 7 days. (C) 3xTg-AD mice (AD) were crossed to SREBP2$^{fl/fl}$ GFAP-Cre$^{+/-}$ mice (AD x SB2$^{-/-}$). Confocal imaging on astrocytes labelled with GFAP (red) and FDFT1 (green) demonstrates down-regulation of the cholesterol synthesis pathway in AD x SB2$^{-/-}$ astrocytes. (D) Representative images of astrocytes showing a change in morphology and spatial distribution. Analysis of cell volume shows a decrease in astrocyte volume after cholesterol knockdown. Quantitation of astrocyte branches shows a decrease in branch points, branch length and sholl intersections in AD x SB2-/- brains compared to AD brains. (E) Confocal imaging on brain slices of AD x SB2-/- shows a robust decrease in % area double labeled with IBA1 and CD68, suggesting a decrease in activated microglia and macrophages after cholesterol knockdown. (F) qPCR of inflammatory cytokines TNFα. (G) TNFα ELISA on brain tissue shows an increased inflammatory level in AD brains compared to wildtype brains. SB2 knockout in astrocytes of AD (ADxSB2-/-) brains significantly downregulated neuroinflammation. (h) Florescent cholesterol oxidase assay from fixed brain slices. SB2-/- decreases cholesterol in both AD (left) and LPS-treated (right) animals. (i) Filipin cholesterol stain. Values are expressed as mean. Each point is a biological replicate (n=3-6 animals per experiment). Comparison made with a Student's T test; or ANOVA (G) *p≤0.05, **p≤0.01, ****p≤0.0001.

We found that treatment of microglia with apoE and 10% FBS significantly increased TNFα production (Figure 2E). As a control we added LPS, which activates TNFα production in cultured microglia [23]. The effect of apoE required cholesterol and was stronger than LPS incubation alone (Figure 2E), a result consistent with our observation that ACM activates microglia. The purified ApoE3 had <0.1ng/µg endotoxin (LPS) (per manufacturer testing) which is <0.0004 ng/mL final concentration and insignificant compared to the 10 ng/mL LPS we added in the assay.

To directly compare the cholesterol response of microglia with macrophages, we incubated RAW 264.7 macrophages with apoE and cholesterol. We found that the uptake of cholesterol into macrophages with apoE was dramatic, >200% compared to the ~10% increase in cholesterol seen in microglia. The uptake of cholesterol using purified apoE3 was remarkably consistent with the relative increases in cholesterol seen using ACM from activated astrocytes (Figure 2A-B). These results suggest the amount of uptake is regulated by the cell.

In addition to uptake, efflux can regulate the cellular levels of cholesterol. We tested the effect of cholesterol efflux on immune cells function. Efflux of cholesterol in microglia can be induced with a liver X agonist. Liver X protein upregulates the ATP binding cassette (ABC) subfamily G member 1

bioRxiv preprint doi: https://doi.org/10.1101/2022.12.12.520161; this version posted December 13, 2022. The copyright holder for this preprint (which was not certified by peer review) is the author/funder, who has granted bioRxiv a license to display the preprint in perpetuity. It is made available under aCC-BY-NC-ND 4.0 International license.

(ABCG1) transporter among other genes. ABCG1 activation was recently reported to downregulate neuropathic pain [24]. In macrophages ABC subfamily A member 1 (ABCA1) effluxes cholesterol.

We treated RAW264.7 macrophages with the Liver X receptor agonist T0901317 and measured cholesterol levels using the fluorescent cholesterol oxidase assay.We saw a 20% decrease in macrophage cholesterol (Figure 2G) which corresponded to a ~10% decrease in TNFα levels (Figure 2H). This suggest genetic regulation of cholesterol levels in microglia affects cytokine production.

In vivo role of astrocyte-derived cholesterol in neuroinflammation

If astrocyte cholesterol facilitates neuroinflammation, then knocking out astrocyte cholesterol *in vivo* should block or reduce neuroinflammation. To test this hypothesis, we injected control (SREBP2flox) and astrocyte specific SREBP2 null (SB2-/-) mice with a single 2 mg/kg dose of LPS and examined microglia activation in the brains of these animals after 7 days (Figure 3A), (Supplemental Figure 1B). To quantitate microglia activation, we measured CD68 levels in IBA1+ cells by confocal immunofluorescence. IBA1 is a marker of microglia and macrophages in the brain. Increases in CD68 levels are commonly observed in neuroinflammatory and neurodegenerative conditions and they are used as a marker of neuroinflammation [252627].The cholesterol-depleted model uses the human GFAP promoter to drive the expression of Cre recombinase in astrocytes to delete SREBP2 (SB2), which we recently developed and characterized to decrease astrocyte cholesterol in the brain [28]. Loss of SB2 from astrocytes has minimal impact on ApoE expression in the brain or secretion into the CSF (Figure S3).

After 7 days, we observed that LPS-injected SB2-/- mice have significantly less CD68 in IBA1+ cells compared to LPS-injected SB2 flox controls (Figure 3B), suggesting decreased astrocyte cholesterol helps resolve neuroinflammation. In agreement, cholesterol levels were decreased in LPS-treated SB2-/- mice (Figure 3H). In contrast, after two 5 mg/kg of LPS treatment and no time for recoverly (day 1) SB2-/- mice exhibited the same microgliosis as LPS treated control animals (Supplemental Figure S2).

Astrocyte cholesterol and neuroinflammation in an AD mouse model.

As mentioned, brain inflammation is a well-established component of Alzheimer's disease and also observed in mouse models of the disease [1]. To test a potential role for astrocyte cholesterol in an AD mouse model, we examined microgliosis in a familial transgenic (3xTg) mouse model of AD [29]. We crossed 3xTg-AD mice with our SREBP2$^{flox/flox}$ GFAP-Cre mice described above to generate an AD mouse model lacking astrocyte cholesterol [17]. We visualized astrocytes using GFAP labelling and also measured the critical cholesterol synthesis enzyme FDFT1 (3C).

As expected FDFT1 was reduced in SB2-/- astrocytes and morphology was clearly altered. Analysis of 3D reconstructions of the hippocampal astrocytes demonstrated significant decreases in SB2-/- astrocyte volume and number of sholl intersections (Figure 3D).

We next immunostained these brains for IBA1 and CD68 proteins to assess the immune activation of the hippocampal microglia and infiltrating macrophages. IBA1 and CD68 imaging showed a robust decrease in the ADxSB2-/- brains (Figure 3E) and the %IBA1 area labeled with CD68 was also significantly decreased in ADxSB2-/- brains compared with AD brains, suggesting a knockdown in astrocyte cholesterol decreases the activation of microglia and macrophages.

To confirm knockout of the astrocyte cholesterol reduced inflammatory cytokine release in vivo, we measured the mRNA level of TNFα, an inflammatory cytokine. As expected, we found TNFα mRNA levels were significantly lower in ADxSB2-/- brains compared to AD brains (Figure 3F). We confirmed that the change in mRNA levels resulted in a change in TNFα protein level using ELISA. With astrocyte cholesterol, the AD brains had significantly higher TNFα level compared to WT control (Figure 3G). Without astrocyte cholesterol, TNFα levels were reduced to that of WT control brains (Figure 3G), suggesting decreased neuroinflammation. Other cytokines, including IL1β, IL1α, INFA and INFB, showed the same trend in mRNA levels, although the differences did not reach statistical significance (Figure S3B-E).

We also tested cholesterol levels in the brain tissue of SB2-/- animals using either a fluorescent cholesterol oxidase assay or a filipin

bioRxiv preprint doi: https://doi.org/10.1101/2022.12.12.520161; this version posted December 13, 2022. The copyright holder for this preprint (which was not certified by peer review) is the author/funder, who has granted bioRxiv a license to display the preprint in perpetuity. It is made available under aCC-BY-NC-ND 4.0 International license.

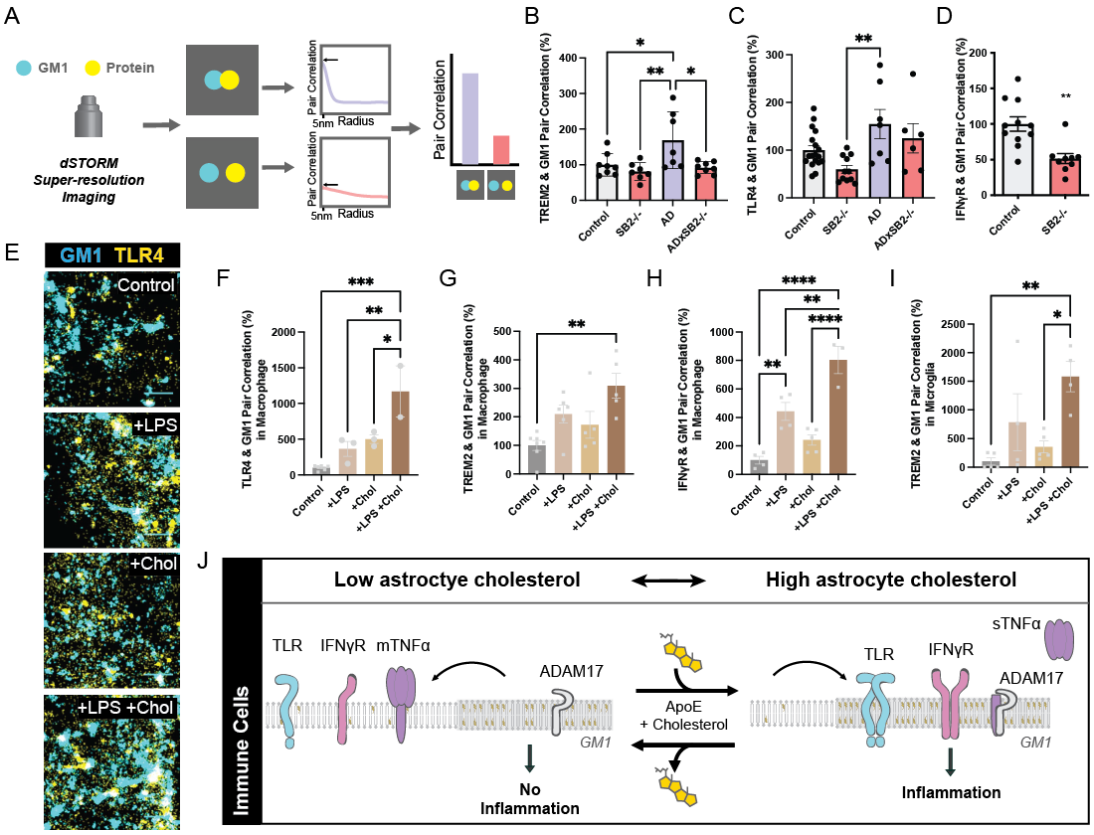

Figure 4. Astrocyte cholesterol clusters inflammatory proteins in microglia and macrophages. (A) Experimental setup and analysis for two color dSTORM. GM1 lipid and protein were fluorescently labeled and their localizations determined by dSTORM. High correlation at short distances (5-10 nm) is graphed and indicates co-localization. (B-D) dSTORM super resolution imaging on brain slices. Compared to healthy animals (white shading), SB2-/- significantly decreased inflammatory clustering of TREM2, TLR4, and INFyR. In 3xTG AD flox (control, purple shading) clustering was dramatically increased. The clustering of TREM2 was reversed in AD animals with astrocyte SREBP2 knockout (AD x SB2-/-) (red shading). (C) TLR4 traffics in the membrane similar to TREM2. (D) IFNγR moves out of GM1 clusters after SB2 KO in astrocytes. Imaging of cholesterol clustering of inflammatory receptors in cultured immune cells. (E-I) LPS treatment or cholesterol loading alone shows a trend in increasing inflammation receptor (TLR4, IFNγR and TREM2), GM1 lipid cluster association. LPS and cholesterol together has an additive effect. (J) The GM1 lipid raft is the platform to initiate inflammatory signaling. LPS or cholesterol is able to move the inflammatory receptors, including TLR, IFNγR and TREM2, to the GM1 lipid clusters, inducing dimerization of the receptors and initiating inflammatory signaling. Cholesterol efflux disrupts GM1 clusters and moves inflammatory receptors out of GM1 clusters into disordered regions, inhibiting inflammatory signaling. Values are expressed as mean each. B-D each point is a cell from 2 experimental brains (4 animals), done in duplicate. F-I each point is a biological replicate (single cell) and comparison are made from samples prepared at the same time. Each experiment was done at least in duplicate. Statistical comparison made with a Student's T test or ANOVA (B,C); *p≤0.05, **p≤0.01, ***p≤0.001, ****p≤0.0001.

stain. Using the cholesterol oxidase assay, SB2-/- animals (day 7) had ~20% less cholesterol (Figure 3H) compared to SB2flox control animals after treatment with 2 mg/Kg LPS. Likewise, the SB2-/- animals had significantly less cholesterol (<30%) when crossed to 3xTG AD animals compared to 3xTG AD animals alone. Similar to the cholesterol oxidase assay, filipin staining showed a significant reduction in staining in brain slices from SB2-/- animals treated with LPS (Figure 3i). 3xTG AD animals also had reduced staining, but the decrease did not reach statistical significance (p=0.28).

Molecular contribution of astrocytes to neuroinflammation.

Lastly, we investigated the effect of astrocyte cholesterol on the state of inflammatory markers. Previous studies suggest that cholesterol clusters inflammatory proteins into lipid domains on the plasma membrane which serves as a platform to activate inflammatory proteins through dimerization and substrate presentation [12,14]. We used

bioRxiv preprint doi: https://doi.org/10.1101/2022.12.12.520161; this version posted December 13, 2022. The copyright holder for this preprint (which was not certified by peer review) is the author/funder, who has granted bioRxiv a license to display the preprint in perpetuity. It is made available under aCC-BY-NC-ND 4.0 International license.

inflammatory receptor association with GM1 lipid clusters as an early upstream marker of *in vivo* neuroinflammation using two-color super-resolution imaging.

Super resolution imaging has emerged as a suitable technique to study cluster-associated proteins by imaging membrane proteins and lipids directly in a native cellular environment [30]. We recently employed super-resolution imaging to establish membrane-mediated mechanisms of anesthesia and amyloid production [3117]. Here we use super-resolution direct stochastical optical reconstruction microscopy (dSTORM) to analyze the co-localization of inflammatory receptors with GM1 lipid clusters (Figure 4A), including, TLR4 and TREM2 and IFNγR in cultured immune cells activated with either cholesterol or LPS or in AD brain tissue.

We found more TREM2 localized with GM1 lipid clusters in the AD brains compared to the WT control (Figure 4B-D), suggesting that high brain cholesterol in these animals correlates with increased inflammatory molecule clustering *in vivo*. Cholesterol knockdown in AD brains decreased TREM2's GM1 association. We observed a similar trend in TLR4's association with GM1 lipids. For IFNγR, ADxSB2-/- brains had a robustly lower GM1 association compared to AD brains.

To confirm cholesterol effects *in vitro*, we treated cultured microglia and macrophages with apoE and measured colocalization of inflammatory receptors with GM1 lipids. We found LPS and cholesterol together had an additive effect (4F-H). Interestingly, mutations in TREM2 have been identified as major risk factors for sporadic Alzheimer's disease (AD). We also confirmed TREM2's translocation into GM1 clusters with LPS and cholesterol in microglia (Figure 4I). Collectively, we show that cholesterol and LPS cluster inflammatory receptors into the GM1 lipids and activate inflammatory signaling (Figure 4J).

Discussion

Abnormal lipid accumulation in neurodegeneration was first observed more than 100 years ago by Alois Alzheimer [32]. Alzheimer described an extensive accumulation of 'adipose saccules' in the patient's brain, which is a major store of cholesterol and fatty acids [33]. We propose a cholesterol-based interplay among astrocytes, microglia, and macrophages in the regulation of neuroinflammation. Figure 2I shows a proposed cellular model based on our findings here. Cytokines, either from the periphery or brain, activate cholesterol synthesis in astrocytes. Astrocytes secrete the cholesterol. Nearby microglia and macrophages sense high extracellular cholesterol and take up the cholesterol. The increased cholesterol drives an inflammatory response causing the release of more cytokines.

The dSTORM used here is an important technical advancement. First, we measured an inflammatory state using the clustering of inflammatory receptors. The signal is direct from the tissue and at the source. Most inflammation is measured by downstream effectors such as RNA expression,but these are complicated by a myriad of downstream inputs that don't necessarily indicate the original inflammatory state in the tissue of interests. While RNA expression and ELISA are valuable tools, particularly when there is robust inflammation, such as with infection, dSTORM imaging is likely to better reveal early or low-grade chronic inflammation.—In time dSTORM may be a preferred method of determining an early inflammatory signal.

Second, we have directly labeled the lipids and compared the protein localization to the signature lipid (GM1). Fluorescent probes targeted to GM1 lipids with palmitate are insufficient as the palmitoylated proteins can leave the GM1 domain when cholesterol conditions change[34]. Hence the ability to function as a GM1 sensor is lost. By directly labeling the lipid, we are able to determine nanoscopic trafficking in the membrane. It is the nanoscopic movement that appears to control the inflammation.

Aspects of cholesterol's regulatory role in the brain mirrors that of the periphery [13,35]. Astrocytes serve the function of the liver cells; i.e., astrocytes respond to cytokines by producing cholesterol (Supplemental Figure S1B). The microglia contribute to the function of macrophages, which take up the cholesterol and escalate the signal in both the brain and the peripheral tissue. In both systems, cholesterol is secreted and transported by lipoproteins to the target immune cell.

Adding astrocytes (Figure 2A) to cultured microglia resulted in a response exactly opposite that of isolated microglia (Figure 2C). This result suggests cultured microglia likely require astrocytes to recapitulate an *in vivo* environment. Others have also seen that co-cultures with astrocytes and microglia better recapitulate *in vivo* studies, despite a lack of mechanistic understanding [36]. In our experiments, we saw

bioRxiv preprint doi: https://doi.org/10.1101/2022.12.12.520161; this version posted December 13, 2022. The copyright holder for this preprint (which was not certified by peer review) is the author/funder, who has granted bioRxiv a license to display the preprint in perpetuity. It is made available under aCC-BY-NC-ND 4.0 International license.

similar results using cholesterol derived from either serum or astrocytes (Figure 2E-F and Figure 4E-G). However, other minor lipid components are transported by apoE and they could in theory result in some differences between serum and astrocyte treatment that we were unable to detect in culture.

The ability of SB2-/- to reduce the total brain cholesterol relative to control in both the AD model and the LPS model is striking (Fig. 3H-I). In the AD model we previously showed a similar striking decrease in both amyloid plaque formation and Tau phosphorylation in the same SB2-/- animals [17]. In the same study we showed the transport of cholesterol from astrocytes to neurons required apoE, suggesting the signal is coming from lipoproteins, not exosomes.

We did not see appreciable differences in whole brain cholesterol levels between the untreated SB2-/- vs. control SB2 flox mice. Using either the cholesterol oxidase assay or filipin staining, SB2-/- tissue showed a slight, but not significant, increase in cholesterol (supplemental Figure S3F-J). The original characterization of the SB2-/- mice likewise saw very little changes in brain cholesterol [28]. This result is significant for two reasons. One, it suggests that under basal conditions non-astrocyte cells are able to maintain cholesterol levels in the brain. And two, astrocyte cholesterol appears to be selectively important for an inflammatory response. In some sense the result is fortuitous, since it allowed us to examine what appears to be inflammatory cholesterol separate from basal cholesterol.

LPS treatment in the periphery is known to open the BBB, which appears to allow LPS to cross [37]. LPS is hydrophobic, so this likely occurs bound to a lipoprotein. Our previous studies showed that microglia are unable to compensate for loss of astrocyte cholesterol in the AD mouse model [17] suggesting a peripheral factor like cholesteol likely crossed into the brain to initiate the acute inflammatory phase after LPS challenge in SB2-/- mice with 5 mg/kg treatment. This conclusion is supported by the decreased TNFα (Figure 3F-G) and decreased TREM2 clustering (Figure 4B) in SB2-/- AD mice and by previous studies that show 10 mg/kg LPS allows immune cell infiltration into the brain[38]. Recently, passage of cholesterol bound lipoproteins through the BBB was hypothesized as a potential instigator of neuro-inflammation[39].

If the BBB opens and then seals, this would nicely explain why we saw no difference in microglia activation in SB2-/- after 1 day (Figure S3). After 7 days, at a lower dose (2 mg/kg), we clearly saw a decrease in microglial activation (Figure 3A). We did not test day 1 at the lower concentration, so it is unclear how much the BBB opened and resealed at 7 days or if the lower dose was insufficient to open the BBB in a SB2-/- mouse. Nonetheless, the significant decrease of inflammation in the SB2-/- animals after 7 days strongly suggests lowering astrocyte cholesterol helps resolve neuroinflammation over time.

Several studies have shown that exposure to a high-fat diet (HFD) can increase microglial activation in the CNS, even without activating peripheral inflammation [4041]. In fact, recent work has shown that only 3 days of HFD exposure is sufficient to promote gliosis in the hypothalamus [42]. This further suggests that peripheral cholesterol itself, or a product downstream of the cholesterol, is getting into the brain.

At the molecular level, cholesterol's primary signaling role is to cluster proteins including inflammatory receptors (e.g., TLR4, TREM2, and IFNγR). As mentioned, this can lead to clustering of inflammatory proteins in microglia and macrophages [12] (Figure 4J). In the AD mouse model, TREM2 clustering was significantly increased and then decreased when crossed with SB2-/-. Clustering of TLR4 was also increased in the AD mouse, but the ability of SB2-/- to reverse the increase was moderate compared to TREM2 (Figure 4C). While cholesterol is a major contributor to clustering of TRL4 and TREM2, other factors (e.g., PIP_2 localization, sensitivity to mechanical force, and membrane disruptive molecules) oppose clustering [14,31] and may help set unique thresholds for each protein in combination with cholesterol. Ultimately, the sum total of the localization factors gives rise to protein activation. The localization effect is a rapid mechanism (<10ms) to dramatically change the concentration of proteins available for signaling [14,30].

Future *in vivo* studies will need to identify the source of inflammation entering the brain through the periphery and the possible role of macrophages in responding to BBB opening. And studies on cultured cells will need to consider high and low cholesterol environments. In order to recapitulate a disease state, cholesterol will likely need to be elevated [21,22]. Lastly, if the cytokines generated from microglia have access to the same astrocytes that produce their cholesterol, the process would be autocatalytic and produce a chain reaction that would escalate neuroinflammation.

bioRxiv preprint doi: https://doi.org/10.1101/2022.12.12.520161; this version posted December 13, 2022. The copyright holder for this preprint (which was not certified by peer review) is the author/funder, who has granted bioRxiv a license to display the preprint in perpetuity. It is made available under aCC-BY-NC-ND 4.0 International license.

Bibliography

1. Guzman-Martinez, L. *et al.* Neuroinflammation as a common feature of neurodegenerative disorders. *Front. Pharmacol.* **10**, 1–17 (2019).
2. DiSabato, D. J., Quan, N. & Godbout, J. P. Neuroinflammation: the devil is in the details. *J. Neurochem.* **139**, 136–153 (2016).
3. Heneka, M. T. *et al.* Neuroinflammation in Alzheimer's disease. *Lancet Neurol.* **14**, 388–405 (2015).
4. Leng, F. & Edison, P. Neuroinflammation and microglial activation in Alzheimer disease: where do we go from here? *Nat. Rev. Neurol.* **17**, 157–172 (2021).
5. Calsolaro, V. & Edison, P. Neuroinflammation in Alzheimer's disease: Current evidence and future directions. *Alzheimer's Dement.* **12**, 719–732 (2016).
6. Fernández-Castañeda, A. *et al.* Mild respiratory COVID can cause multi-lineage neural cell and myelin dysregulation. *Cell* **185**, 2452-2468.e16 (2022).
7. Matejuk, A. & Ransohoff, R. M. Crosstalk Between Astrocytes and Microglia: An Overview. *Front. Immunol.* **11**, 1–11 (2020).
8. Jha, M. K., Jo, M., Kim, J. H. & Suk, K. Microglia-Astrocyte Crosstalk: An Intimate Molecular Conversation. *Neuroscientist* **25**, 227–240 (2019).
9. Kwon, H. S. & Koh, S. H. Neuroinflammation in neurodegenerative disorders: the roles of microglia and astrocytes. *Transl. Neurodegener.* **9**, 1–12 (2020).
10. Wang, C. *et al.* Selective removal of astrocytic APOE4 strongly protects against tau-mediated neurodegeneration and decreases synaptic phagocytosis by microglia. *Neuron* 1–18 (2021). doi:10.1016/j.neuron.2021.03.024
11. Martín, M. G., Pfrieger, F. & Dotti, C. G. Cholesterol in brain disease: sometimes determinant and frequently implicated. *EMBO Rep.* **15**, 1036–1052 (2014).
12. Miller, Y. I., Navia-Pelaez, J. M., Corr, M. & Yaksh, T. L. Lipid rafts in glial cells : Role in neuroinflammation and pain processing. *J. Lipid Res.* **61**, 1–23 (2020).
13. Tall, A. R. & Yvan-Charvet, L. Cholesterol, inflammation and innate immunity. *Nat. Rev. Immunol.* **15**, 104–116 (2015).
14. Petersen, E. N., Chung, H.-W., Nayebosadri, A. & Hansen, S. B. Kinetic disruption of lipid rafts is a mechanosensor for phospholipase D. *Nat. Commun.* **7**, 13873 (2016).
15. Loving, B. A. & Bruce, K. D. Lipid and Lipoprotein Metabolism in Microglia. *Front. Physiol.* **11**, 1–20 (2020).
16. Björkhem, I., Meaney, S. & Fogelman, A. M. Brain Cholesterol: Long Secret Life behind a Barrier. *Arterioscler. Thromb. Vasc. Biol.* **24**, 806–815 (2004).
17. Wang, H. *et al.* Regulation of beta-amyloid production in neurons by astrocyte-derived cholesterol. *Proc. Natl. Acad. Sci.* **118**, e2102191118 (2021).
18. Feingold, K. R. *et al.* Multiple cytokines stimulate hepatic lipid synthesis in vivo. *Endocrinology* **125**, 267–74 (1989).
19. Sevenich, L. Brain-resident microglia and blood-borne macrophages orchestrate central nervous system inflammation in neurodegenerative disorders and brain cancer. *Front. Immunol.* **9**, 1–16 (2018).
20. Kamma, E., Lasisi, W., Libner, C., Ng, H. S. & Plemel, J. R. Central nervous system macrophages in progressive multiple sclerosis: relationship to neurodegeneration and therapeutics. *J. Neuroinflammation* **19**, 1–27 (2022).
21. Wang, H., Yuan, Z., Pavel, M. A. & Hansen, S. The role of high cholesterol in aged related COVID19 lethality. *bioRxiv* 2020.05.09.086249 (2020). doi:10.1101/2020.05.09.086249
22. Yuan, Z. *et al.* Hydroxychloroquine blocks SARS-CoV-2 entry into the endocytic pathway in mammalian cell culture. *Commun. Biol.* **5**, 958 (2022).
23. Sawada, M., Kondo, N., Suzumura, A. & Marunouchi, T. Production of tumor necrosis factor-alpha by microglia and astrocytes in culture. *Brain Res.* **491**, 394–7 (1989).
24. Navia-Pelaez, J. M. *et al.* Normalization of cholesterol metabolism in spinal microglia alleviates neuropathic pain. *J. Exp. Med.* **218**, (2021).
25. Nagamoto-Combs, K., McNeal, D. W., Morecraft, R. J. & Combs, C. K. Prolonged microgliosis in the rhesus monkey central nervous system after traumatic brain injury. *J. Neurotrauma* **24**, 1719–1742 (2007).
26. Owlett, L. D. *et al.* Gas6 induces inflammation and reduces plaque burden but worsens behavior in a sex-dependent manner in the APP/PS1 model of Alzheimer's disease. *J. Neuroinflammation* **19**, 1–17 (2022).
27. Hoogland, I. C. M., Houbolt, C., van Westerloo, D. J., van Gool, W. A. & van de Beek, D. Systemic inflammation and microglial activation: Systematic review of animal experiments. *J. Neuroinflammation* **12**, 1–13 (2015).
28. Ferris, H. A. *et al.* Loss of astrocyte cholesterol synthesis disrupts neuronal function and alters whole-body metabolism. *Proc. Natl. Acad. Sci. U. S. A.* **114**, 1189–1194 (2017).
29. Oddo, S. *et al.* Triple-transgenic model of Alzheimer's disease with plaques and tangles: intracellular Abeta and synaptic dysfunction. *Neuron* **39**, 409–421 (2003).
30. Robinson, C. V., Rohacs, T. & Hansen, S. B. Tools for Understanding Nanoscale Lipid Regulation of Ion Channels. *Trends Biochem. Sci.* **44**, 795–806 (2019).
31. Pavel, M. A., Petersen, E. N., Wang, H., Lerner, R. A. & Hansen, S. B. Studies on the mechanism of general anesthesia. *Proc. Natl. Acad. Sci. U. S. A.* **117**, 13757–13766 (2020).
32. Stelzmann, R. A., Norman Schnitzlein, H. & Reed Murtagh, F. An english translation of alzheimer's 1907 paper, "über eine eigenartige erkankung der hirnrinde". *Clin. Anat.* **8**, 429–431 (1995).
33. Farmer, B. C., Walsh, A. E., Kluemper, J. C. & Johnson, L. A. Lipid Droplets in Neurodegenerative Disorders. *Front. Neurosci.* **14**, 1–13 (2020).
34. Zacharias, D. A., Violin, J. D., Newton, A. C. & Tsien, R. Y. Partitioning of lipid-modified monomeric GFPs into

bioRxiv preprint doi: https://doi.org/10.1101/2022.12.12.520161; this version posted December 13, 2022. The copyright holder for this preprint (which was not certified by peer review) is the author/funder, who has granted bioRxiv a license to display the preprint in perpetuity. It is made available under aCC-BY-NC-ND 4.0 International license.

membrane microdomains of live cells. *Science* **296**, 913–6 (2002).
35. Luo, J., Yang, H. & Song, B. L. Mechanisms and regulation of cholesterol homeostasis. *Nat. Rev. Mol. Cell Biol.* **21**, 225–245 (2020).
36. Goshi, N., Morgan, R. K., Lein, P. J. & Seker, E. A primary neural cell culture model to study neuron, astrocyte, and microglia interactions in neuroinflammation. *J. Neuroinflammation* **17**, 1–16 (2020).
37. Vargas-Caraveo, A. *et al.* Lipopolysaccharide enters the rat brain by a lipoprotein-mediated transport mechanism in physiological conditions. *Sci. Rep.* **7**, 1–15 (2017).
38. Mouton, P. R. *et al.* The effects of age and lipopolysaccharide (LPS)-mediated peripheral inflammation on numbers of central catecholaminergic neurons. *Neurobiol. Aging* **33**, 423.e27-423.e36 (2012).
39. Rudge, J. D. A. A New Hypothesis for Alzheimer's Disease: The Lipid Invasion Model. *J. Alzheimer's Dis. Reports* **6**, 129–161 (2022).
40. Ziko, I. *et al.* Neonatal overfeeding alters hypothalamic microglial profiles and central responses to immune challenge long-term. *Brain. Behav. Immun.* **41**, 32–43 (2014).
41. Kang, E. B. *et al.* Neuroprotective Effects of Endurance Exercise Against High-Fat Diet-Induced Hippocampal Neuroinflammation. *J. Neuroendocrinol.* **28**, (2016).
42. Thaler, J. P. *et al.* Obesity is associated with hypothalamic injury in rodents and humans. *J. Clin. Invest.* **122**, 153–162 (2012).
43. Petersen, E. N., Pavel, M. A., Wang, H. & Hansen, S. B. Disruption of palmitate-mediated localization; a shared pathway of force and anesthetic activation of TREK-1 channels. *Biochim. Biophys. Acta - Biomembr.* **1862**, 183091 (2020).
44. Lang, T. *et al.* SNAREs are concentrated in cholesterol-dependent clusters that define docking and fusion sites for exocytosis. *EMBO Journal* **20**, 2202–2213 (2001).
45. Tellier, E. *et al.* The shedding activity of ADAM17 is sequestered in lipid rafts. *Exp. Cell Res.* **312**, 3969–3980 (2006).
46. Levental, I., Lingwood, D., Grzybek, M., Coskun, U. & Simons, K. Palmitoylation regulates raft affinity for the majority of integral raft proteins. *Proc. Natl. Acad. Sci.* **107**, 22050–22054 (2010).
47. German, C. L., Gudheti, M. V., Fleckenstein, A. E. & Jorgensen, E. M. Brain slice staining and preparation for three-dimensional super-resolution microscopy. in *Methods in Molecular Biology* (2017). doi:10.1007/978-1-4939-7265-4_13

Acknowledgements

We thank Julian Bois for help with the cholesterol assays and Allan Tall for reading of the manuscript and helpful suggestions. We thank Tajie Harris for assistance with CSF experiments. This work was supported by the NIH via an R21 (Grant R21 AG078845-01), Director's New Innovator Award (DP2NS087943), and R01 (Grant R01NS112534) to S.B.H., a K08 (Grant K08DK097293) and Owens Family Foundation Award to H.A.F., and a NIH T32 (Grant T32DK764627) to J.A.K. We are grateful to the JPB Foundation for the purchase of a super resolution microscope.

bioRxiv preprint doi: https://doi.org/10.1101/2022.12.12.520161; this version posted December 13, 2022. The copyright holder for this preprint (which was not certified by peer review) is the author/funder, who has granted bioRxiv a license to display the preprint in perpetuity. It is made available under aCC-BY-NC-ND 4.0 International license.

Supplementary Information
Discussion

For our studies the localization of the proteins dictates their function. The location was determined by fixing the cells and measuring pair correlation of the protein with the lipid. The lipids are relatively small and they are best labeled with antibodies or, in the case of GM1 lipids, with cholera toxin B (CTxB). CTxB is pentadentate which is why the label has very high affinity to a small lipid. The labeling can cause some clustering even when fixed prior to labeling. We have seen very minimal clustering in our setup in multiple cell types [43]. Nonetheless, artificial clustering does not adversely affect localization of proteins since it has very little effect on where a protein is localized. In fact, in 2003 Reinhard Jahn intentionally used clustering of unfixed cells to help define if proteins were colocalized or not. He called this “antibody patching”. In short, he induced the clustering and then looked to see which proteins clustered with the different “patches” of antibodies [44]. The patching was necessary since at the time they didn’t have super resolution imaging. It is evident from those studies that even if there is some residual clustering after we fix, that is very unlikely to affect the relative localization of fixed proteins. Since our conclusions are based off of pair correlation and localization, not size, any putative clustering by CTxB is likely desirable for determining an accurate result.

bioRxiv preprint doi: https://doi.org/10.1101/2022.12.12.520161; this version posted December 13, 2022. The copyright holder for this preprint (which was not certified by peer review) is the author/funder, who has granted bioRxiv a license to display the preprint in perpetuity. It is made available under aCC-BY-NC-ND 4.0 International license.

Supplementary Figures

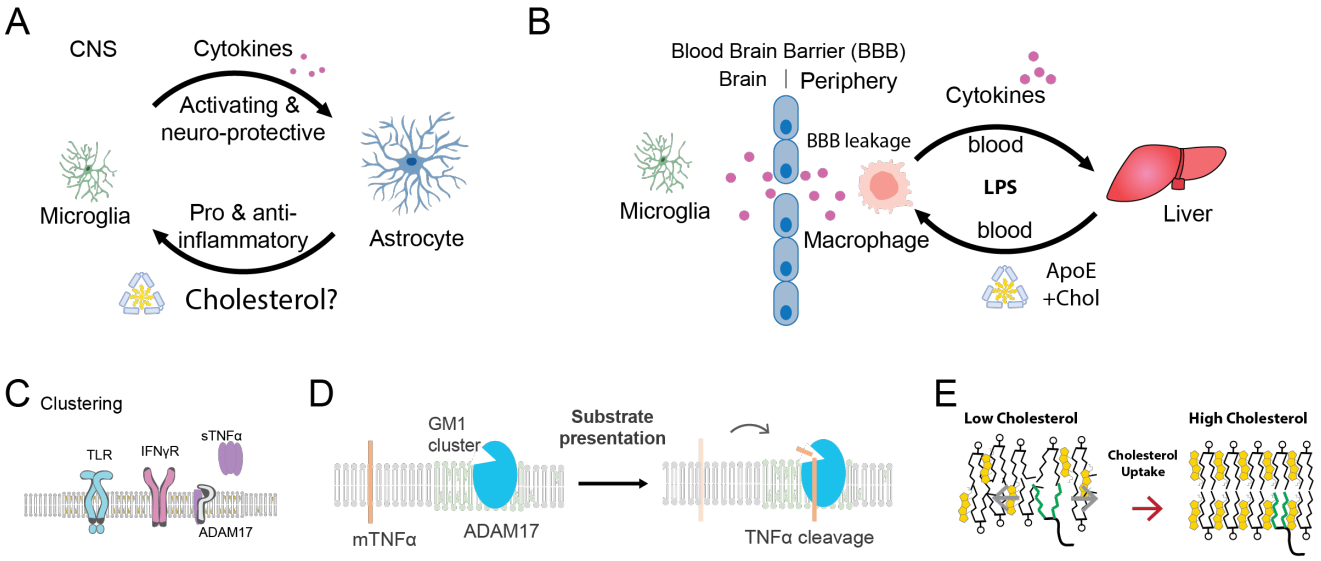

Figure S1. Molecules of Neuroinflammation. (A) Communication between microglia and astrocytes. Astrocytes (blue shaded cell) and microglia (green shaded cell) interact by releasing signaling factors locally, known as paracrine signaling. Microglia primarily release cytokines. Astrocytes release both pro and anti-inflammatory factors [7]. Cholesterol (yellow shading) is drawn in a complex with apolipoprotein E (apoE, light blue shading). The current study asks if astrocytes produce cholesterol that makes its way to microglia and is this a signal in microglia? (B) Inflammation in the CNS is influenced by the periphery. Lipopolysaccharide (LPS) and cytokines induce cholesterol synthesis in the liver. The liver produces cholesterol which is secreted and transported in the blood in lipoprotein particles containing apolipoprotein E (apoE) and other lipoproteins (not shown). ApoE binding to cell surface receptors on macrophages (not shown) and uptake of the cholesterol activates the macrophages in the periphery, producing cytokines. Through poorly understood mechanisms, LPS in the periphery can activate microglia in the CNS. (C) A representation of cytokine receptors regulated by clustering in lipid rafts. Cholesterol induces clustering of inflammatory proteins. In the case of toll-like receptor (TLR) the clustering causes dimers to form and this leads to autophosphorylation. In the case of tumor necrosis factor alpha (TNFα) a membrane tethered TNFα (mTNFα) clusters with its hydrolytic enzyme ADAM17 where the enzyme is able to catalyze the production of soluble TNFα (sTNFα). sTNFα can then signal inflammation. D) Substrate presentation is a biological mechanism that activates a protein by gaining access to its substrate [14] (e.g., ADAM17 accessing mTNFα) [45](E) Molecular basis for cholesterol's ability to cluster palmitoylated proteins. Cholesterol orders the acyl chains of saturated lipids. The order is thought to create a low energy state. The order of the lipids creates a binding site for palmitates. The cell covalently attaches palmitates to proteins in a process called palmitoylation and the palmitoylation imbues the protein with an affinity for cholesterol dependent ordered lipids [46]. Increasing cholesterol in the membrane increases the number of palmitate binding sites and drives proteins to cluster with GM1 lipids.

bioRxiv preprint doi: https://doi.org/10.1101/2022.12.12.520161; this version posted December 13, 2022. The copyright holder for this preprint (which was not certified by peer review) is the author/funder, who has granted bioRxiv a license to display the preprint in perpetuity. It is made available under aCC-BY-NC-ND 4.0 International license.

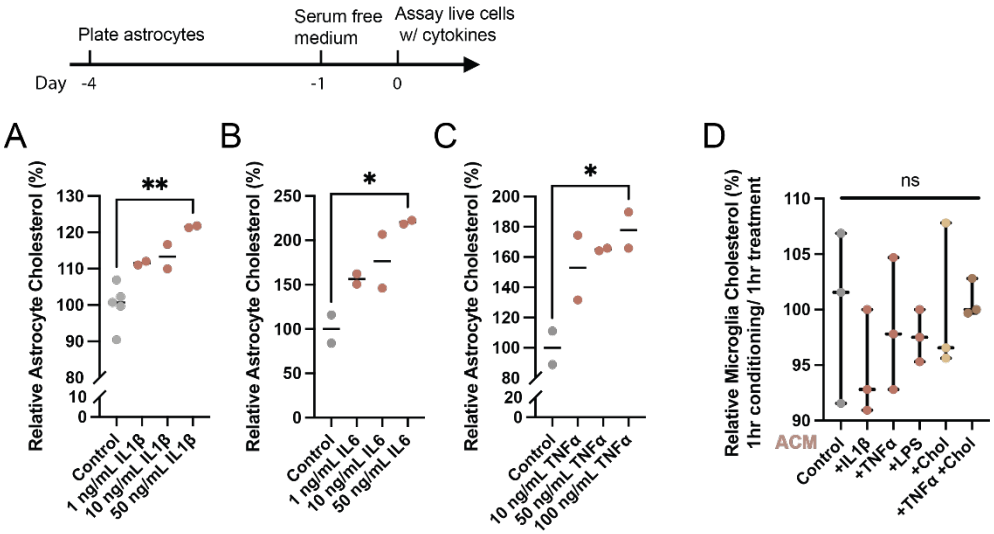

Figure S2 Cytokine dose responses. (A-C) Combined cholesterol from media and available in the plasma membrane measured by a fluorescent cholesterol assay. Pro-inflammatory cytokines IL1β, IL6, and TNFα dose dependently induce cholesterol synthesis in astrocytes. (D) Cytokines (50 nM were added to HMC microglia for 1 hour and the cholesterol measured using a fluorescent cholesterol oxidase assay. Microglia do not respond to cytokines within one hour.

bioRxiv preprint doi: https://doi.org/10.1101/2022.12.12.520161; this version posted December 13, 2022. The copyright holder for this preprint (which was not certified by peer review) is the author/funder, who has granted bioRxiv a license to display the preprint in perpetuity. It is made available under aCC-BY-NC-ND 4.0 International license.

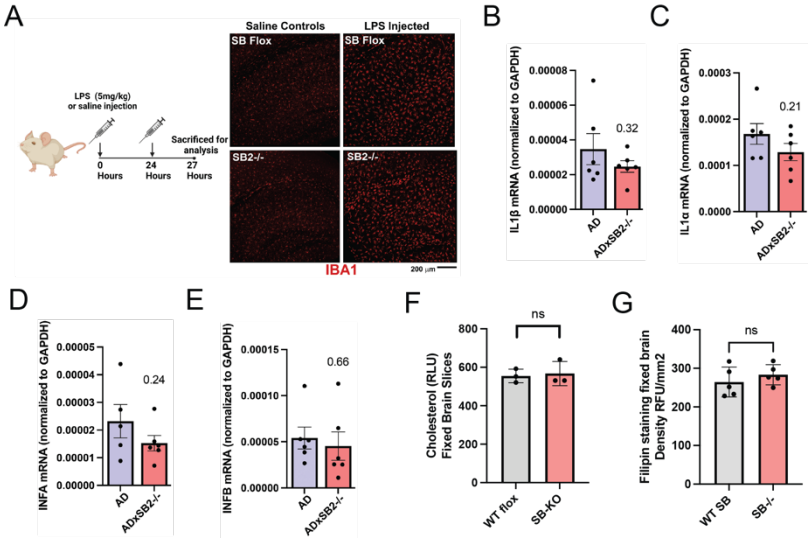

Figure S3. I.P. LPS injection drives microglial activation in SB2 flox (WT control) and astrocyte SB2-/- mice. (A) Mice were I.P. injected 2 times with saline or 5mg/kg LPS dissolved in saline. Brains were harvested 27 hours post-injection and examined for IBA1 immunoreactivity to assess microglial activation. SB2-/- mice demonstrated a similar increase in IBA1 expression in response to LPS. (B-E) qPCR of inflammatory cytokines IL1β (B), IL1α (C), INFA (D) and INFB (E) shows a trend of decreased inflammation in SB2-/- similar to TNFα (see Figure 3F). (F) Cholesterol assay on brain slices from SREBP2 (SB2) flox (WT flox) and SB2-/- mice (in the absence of LPS). Under resting non-inflamed state, SB2-/- has no effect, suggesting that something other than SREBP2 is regulating cholesterol in the non-inflamed state. See Figure 3h for comparison to LPS treated animals. (G) Cholesterol determination as in panel F using Filipin staining. Values are expressed as mean each point is a biological replicate. Comparison made with a Student's T test; p values shown or n.s.= not significant.

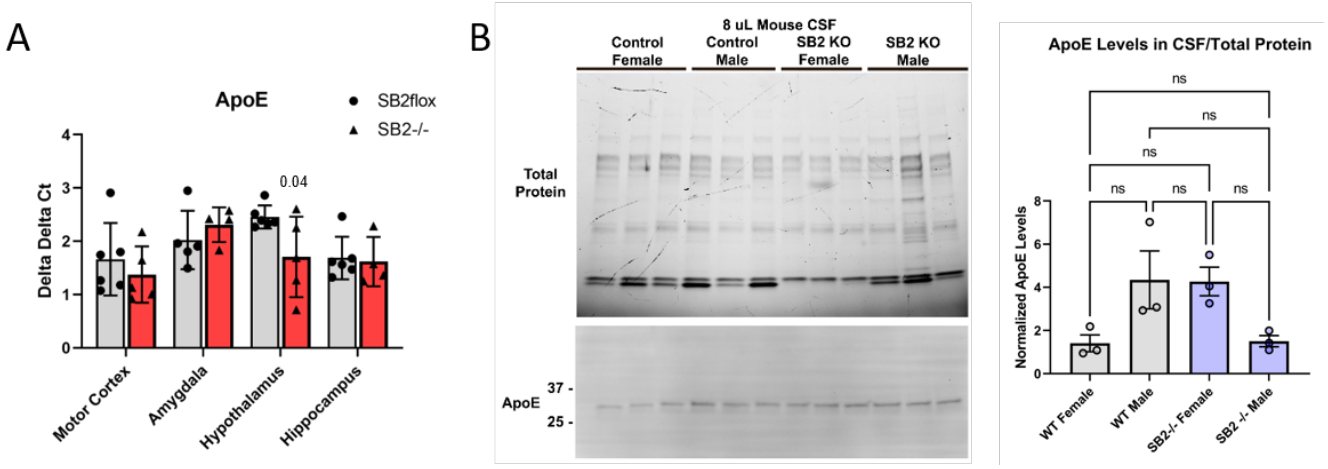

Figure S4. Loss of astrocyte SREBP2 does not impact brain ApoE levels. A. qPCR was performed on brain homogenate from the regions indicated. Values are reported as the delta delta Ct with TBP used as a housekeeping gene. There was a small decrease in hypothalamic ApoE transcription in the hypothalamus of SB2-/- mice but no difference in other brain regions. N= 4-6 animals per region. B. CSF was obtained from SBflox (WT) or SB2 -/- male and female mice. Each data point is the pooled CSF from 2-3 animals. There was no difference in ApoE CSF levels between WT and SB2 -/- mice. Comparison made with a Student's T test in A and ANOVA in B.

bioRxiv preprint doi: https://doi.org/10.1101/2022.12.12.520161; this version posted December 13, 2022. The copyright holder for this preprint (which was not certified by peer review) is the author/funder, who has granted bioRxiv a license to display the preprint in perpetuity. It is made available under aCC-BY-NC-ND 4.0 International license.

Supplemental Methods

Animals

Housing, animal care and experimental procedures were consistent with the Guide for the Care and Use of Laboratory Animals and approved by the Institutional Animal Care and Use Committee of the Scripps Research Institute and the University of Virginia. 3xTg-AD mice and B6129SF2/J controls were purchased from Jackson labs. The 3xTg-AD mice were maintained homozygous for all transgenes. SREBP2$^{flox/flox}$ mice (a generous gift of Dr. Jay Horton at UT Southwestern, now available through Jackson labs) were crossed to the hGFAP-Cre as previously described [28]. These mice were in turn bred to the 3xTg-AD line and crossed back to homozygosity for both the 3xTg-AD transgenes and the SREBP2-flox. 3xTg-AD x SREBP2$^{flox/flox}$ (AD x SB2flox) and 3xTg-AD x SREBP2$^{flox/flox}$ x GFAP-Cre (AD x SB2$^{-/-}$) are littermates. Only female mice were used for the AD crosses as the male 3xTg-AD mice have a much milder phenotype.

Cell culture

RAW 264.7 macrophage cells were grown in Dulbecco's Modified Eagle Medium (DMEM) containing 10% fetal bovine serum (FBS) and 1% penicillin/streptomycin (P/S). Human microglial HMC3 cells were grown in Eagle's Minimum Essential Medium (EMEM) containing 10% FBS and 1% P/S.

Astrocytes were isolated from the cortices of embryonic day 18-21 CD1 mice as described previously[17]. Briefly, cells were dissociated by papain digestion and plated on poly-D-lysine-coated (0.01 mg/mL) tissue culture dish. Dissociated cells were plated in DMEM containing 10% FBS and 1% P/S at 37 °C in 5% CO_2.

LPS IP Injections

LPS IP injections were performed in ~15 week old male mice using 2 doses of 5 mg/kg LPS in saline for acute studies and a single injection of 2 mg/kg LPS for day 7 assessments of microglia activation. LPS was purchased from Sigma Aldrich (L3024) and the same lot of LPS was used for all animals tested. LPS was diluted into sterile saline solution at a concentration of 5 mg/mL. Mice were monitored throughout the course of the experiment and provided with extra cotton nest bedding. Sickness behavior in animals was evident at 24 hours and improved over the course of 5 days.

Astrocyte conditioned media (ACM)

For acute collection of ACM, reactive astrocyte cultures were treated for 1 h with IL-1β (100 ng/ml, Sigma, #SRP8033), TNFα (100 ng/ml, Novus Biologicals, #NBP2-35076), LPS (100 ng/mL, Sigma-Aldrich, #L2018) or loaded with cholesterol using apoE3 (4 μg/mL, BioVision, #4696-500). Endotoxin assayed to be less than 0.1 ng/μg of apoE3 a concentration non-reactive with microglia.

After treatment, astrocytes were incubated with fresh media for 1 h to collect ACM. Microglia and macrophages were incubated with control or reactive ACM for 1 h before cholesterol measurement.

For an elongated collection of ACM, reactive astrocyte cultures were treated for 24 h with either IL-1β (100 ng/ml), IL6 (100 ng/ml, Thermo Fisher Scientific, #PHC0064), and TNFα (100 ng/ml), or LPS (100 ng/mL). After treatment, astrocytes were incubated with fresh media for 24 h to collect ACM. Microglia and macrophages were incubated with control or reactive ACM for 24 h before cholesterol measurement.

dSTORM Super-resolution imaging

Fixed cell preparation

Cells were grown to 60% confluence. Cells were rinsed with PBS and then fixed with 3% paraformaldehyde and 0.1% glutaraldehyde for 15 min to fix both proteins and lipids. Fixative chemicals were reduced by incubating with 0.1% $NaBH_4$ for 7 min with shaking followed by three times 10 min washes with PBS. Cells were permeabilized with 0.2% Triton X-100 for 15 min and then blocked with a standard blocking buffer (10% bovine serum albumin (BSA) / 0.05% Triton in PBS) for 90 min at room temperature. For labelling, cells were incubated with primary antibody (TLR4: Thermo Fisher Scientific, #482300; TREM2: R&D Systems, #MAB17291; IFNγR: Thermo Fisher Scientific, #10808-1-AP) for 60 min in 5% BSA / 0.05% Triton / PBS at room temperature followed by 5 washes with 1% BSA / 0.05% Triton / PBS for 15 min each. Secondary antibody was added in the same buffer as primary for 30 min at room temperature followed by 5 washes as stated above. Cells were then washed with PBS for 5 min. Cell labelling and washing steps were performed while shaking. Labeled cells were then post-fixed with fixing solution, as above, for 10 min without shaking followed by three 5 min washes with PBS and two 3 min washes with deionized distilled water. The specificity of the antibodies used in dSTORM imaging were validated by western blots (see manufacture product page). Specifically, TREM2 antibody stains TREM2 transfectants but not TREM1 transfectants in flow cytometry.

Brain slice preparation

bioRxiv preprint doi: https://doi.org/10.1101/2022.12.12.520161; this version posted December 13, 2022. The copyright holder for this preprint (which was not certified by peer review) is the author/funder, who has granted bioRxiv a license to display the preprint in perpetuity. It is made available under aCC-BY-NC-ND 4.0 International license.

Mouse brain slicing and staining were performed as previously described[47] with minor modifications. Mouse brains were fixed in 4% paraformaldehyde, incubated in a 20% sucrose/PBS solution at 4 °C for 3 days, and embedded in Tissue-Tek OCT compound (Sakura). Sagittal sections (50 µm) were collected and placed into 24-well plate wells containing PBS. Fixative chemicals were reduced by incubating with 0.1% $NaBH_4$ for 30 min while gently shaking at room temperature followed by three times 10 min washes with PBS. Samples were permeabilized with 0.2% Triton X-100 for 2 hours and then blocked with a standard blocking buffer (10% bovine serum albumin (BSA) / 0.05% Triton in PBS) for 6 hours at room temperature. For labelling, samples were incubated with primary antibody for 3 hours in 5% BSA / 0.05% Triton / PBS at room temperature then 3 days at 4 °C followed by 5 washes with 1% BSA / 0.05% Triton / PBS for 1 hour each. Secondary antibody was added in the same buffer as primary for 3 days at 4 °C followed by 5 washes as stated above. Sample labelling and washing steps were performed while shaking. Labeled brain tissues were then post-fixed with fixing solution, as above, for 1 hour without shaking followed by three 30 min washes with PBS and two 30 min washes with deionized distilled water. Brain slices were mounted onto the stainless-steel imaging chamber (Life Sciences, #A-7816) with #1 thickness coverglass (Chemglass, # CLS-1760-025), and 2% agarose were pipetted onto the slice to form a permeable agarose pad and prevent sample movement during imaging.

Quantitation of Astrocyte Morphology and Microglia CD68

Astrocyte cell 3D reconstructions were quantified using IMARIS filament package software. Mouse brain hemispheres were collected from PBS perfused 40 week old animals. Tissue was cut into 40 µm sections and immuno-stained using anti-GFAP antibody (Mab360, EMD Millipore) applied overnight at a 1:500 concentration in a immunostaining blocking solution of 5% BSA, 5% horse serum, 0.1% Triton X-100 in PBS. Alexa 647 secondary antibody was applied for fluorescent visualization. Astrocyte FDFT1 was immuno-stained in complementary experiments using Abcam antibody Ab195046 at a 1:200 dilution. Confocal microscopy Z-stack images of astrocyte populations were collected using a Leica TCS SP8 confocal microscope from the CA1 region of the hippocampus (30 µm depth, 0.5 µm steps, x 20 magnification) of each animal. Raw .tif files were then used for IMARIS software analysis (Oxford Instruments). IMARIS was used to reconstruct the astrocyte (GFAP) surfaces. A threshold of 20/250 was applied to each image before analysis. The reconstruction was used for filament reconstruction using a max diameter of 10.0 µm with seed points at 0.200 µm and a diameter of sphere regions set to 15 µm. Surface and filament parameters from each astrocyte cell population were then exported to excel for statistical analysis in PRISM software. All images taken for analysis were collected in a single imaging session using the same parameters including pinhole, laser intensity and gain.

For determining the CD68 content of hippocampal microglia, 40 µm PFA fixed brain sections from LPS injected animals and 3xTg AD animals (described above) were immuno-stained by applying an IBA1 antibody (E4O4W, Cell Signaling) at a 1:500 dilution and a CD68 antibody (FA-11, Bio Rad) at a 1:500 dilution in blocking solution (described above) overnight at 4 degrees. Alexa Fluor 647 anti rabbit and Alexa Fluor 555 anti-Rat secondary antibodies were used for visualization. Confocal Z-stack images of hippocampal IBA1+ cell populations were collected from each brain section (~36 µm depth, 0.5 µm steps, x 20 magnification) using a Leica Stellaris 8 confocal microscope. Raw .lif files were imported into IMARIS software to perform 3D reconstructions. IBA1 and CD68 were set with a threshold cutoff of 20/250. The colocalization function was then used to determine the % colocalization in the region of interest as well as the % of IBA1 area occupied with CD68. 3 sections from each individual animal were imaged, analyzed and averaged to generate each individual datapoint for statistical analysis.

dSTORM imaging

Images were recorded with a Bruker Vutara 352 with a 60X Olympus Silicone objective. Frames with an exposure time of 20 ms were collected for each acquisition. Excitation of the Alexa Fluor 647 dye was achieved using 640 nm lasers and Cy3B was achieved using 561 nm lasers. Laser power was set to provide isolated blinking of individual fluorophores. Cells were imaged in a photo-switching buffer comprising of 1% β-mercaptoethanol (Sigma, #63689), oxygen scavengers (glucose oxidase (Sigma, #G2133) and catalase (Sigma, #C40)) in 50mM Tris (Affymetrix, #22638100) + 10mM NaCl (Sigma, #S7653) + 10% glucose (Sigma, #G8270) at pH 8.0. Axial sample drift was corrected during acquisition through the Vutara 352's vFocus system.

Images were constructed using the default modules in the Zen software. Each detected event was fitted to a 2D Gaussian distribution to determine the center of each point spread function plus the localization precision. The Zen software also has many rendering options including removing localization errors and outliers based on brightness and size of fluorescent signals. Pair correlation and cluster analysis was performed using the Statistical Analysis package in the Vutara SRX software. Pair Correlation analysis is a statistical method used to determine the strength of correlation between two objects by counting the number of points of probe 2 within a certain donut-radius of each point of probe 1. This allows for localization to be determined without overlapping pixels as done in traditional diffraction-limited microscopy. Cluster size estimation and cluster density were calculated through cluster

bioRxiv preprint doi: https://doi.org/10.1101/2022.12.12.520161; this version posted December 13, 2022. The copyright holder for this preprint (which was not certified by peer review) is the author/funder, who has granted bioRxiv a license to display the preprint in perpetuity. It is made available under aCC-BY-NC-ND 4.0 International license.

analysis by measuring the length and density of the clusters comprising of more than 10 particles with a maximum particle distance of 0.1 µm.

Cholesterol assay

To measure the relative changes in cholesterol level (free cholesterol or total cholesterol), we developed an Amplex Red-based cholesterol assay. Briefly, cells were seeded into 96-well flat culture plates with transparent-bottom to reach confluency (~ 5 x 10^4 per well). After washing with 200 µL of PBS, cholesterol assay reactions were promptly begun by adding 100 µL of working solution containing 50 µM Amplex red, 1 U/mL horseradish peroxidase, 2 U/mL cholesterol oxidase and 2 U/mL cholesterol esterase in PBS. Relative cholesterol concentration and the background (lacking cells) was determined in triplicate for each sample by measuring fluorescence activity with a fluorescence microplate reader (Tecan Infinite 200 PRO, reading from bottom) for 2 hours at 37°C with excitation wavelength of 530 nm and an emission wavelength of 585 nm. Subsequently, cholesterol level was normalized to the control activity. End point cholesterol signals were then graphed (Mean ± s.e.m.) and statistically analyzed (one-way ANOVA) with GraphPad Prism software (v6.0f).

Filipin Staining

Filipin comple (Sigma (F-9765) 25 mg/ml in DMSO was diluted to 0.05 mg/ml in PBS/10% FBS. Brain slices fixed in 4% PFA were rinsed 3x with PBS and incubated with 1 ml of 1.5 mg glycine/ml PBS for 10 min at room temperature. The slices were stained with 1 mL of 0.05 mg/ml flipin working solution for 2h at room temp with slow shaking. The slices were rinsed 3x with PBS and imaged on a FV-1000 Olympus confocal with 20x objective.

ELISA

The ELISA plate (Invitrogen 44-2404-21) was coated with 100 µL anti-mouse TNFα antibody (capture antibody, BioLegend #510802) diluted 1:250 in coating buffer (BioLegend #421701) and incubated overnight at 4°C. The plate was washed with 200 µL PBS for three times, blocked with 100 µL blocking buffer (PBS with 10%BSA and 0.05% TritonX-100), and incubated for 1 h. Then the blocking buffer was removed from each well and 50 µL supernatant was added and incubated for 1 h. Next, 50 µL Biotin anti-mouse TNFα antibody (primary antibody, BioLegend #506312) diluted 1:1000 in PBST buffer (PBS with 0.01% TritonX-100) was mixed with the supernatant and incubated for 3 h. The plate was washed with 200 µL PBST for four times and incubated with 80 µL HRP streptavidin (BioLegend #405210) diluted 1:1000 in PBST for 1 h in the dark. After that, the plate was washed with 200 µL PBST for four times and incubated with 80 µL Chromogen (Invitrogen #002023) for 30 min in the dark. The substrate development was terminated by 80 µL stop solution (Invitrogen #SS04). Relative TNFα concentration was determined by measurement of absorbance at 450nm on a microplate reader (Tecan Infinite 200 PRO).

qPCR on Brain Tissue

RNA was extracted from 60 week old female 3xTg and 3xTgxSB2-/- frontal cortex using the Isolate II RNA Mini Kit (BIO-52073) from Bioline per manufacturer's instructions. cDNA synthesis was performed using the iScript cDNA synthesis kit (#1708841) from Bio Rad using a SimpliAmp thermocycler following iScript manufacturer's instructions with 1 µg input RNA. qPCR was performed by standard protocols using the following TaqMan primers: GAPDH Mm99999915_g1, TNFa Mm00443258_m1, NFKb Mm00476361_m1, IL1b Mm00434228_m1, IL1a Mm00439620_m1, INFa Mm00833961_s1, and INFb Mm00439552_s1. GAPDH served as a loading control for normalization and the relative abundance of transcripts was determined using the 2^-(Target Cq-GAPDH Cq) formula.